International Journal of Mechanical, Industrial and Aerospace Sciences
ISSN: 2517-9950
Vol:14, No:9, 2020

Deployment of a Biocompatible International Space Station into Geostationary Orbit

Tim Falk, Chris Chatwin

Abstract**—**This study explores the possibility of a space station that will occupy a geostationary equatorial orbit (GEO) and create artificial gravity using centripetal acceleration. The concept of the station is to create a habitable, safe environment that can increase the possibility of space tourism by reducing the wide variation of hazards associated with space exploration. The ability to control the intensity of artificial gravity through Hall-effect thrusters will allow experiments to be carried out at different levels of artificial gravity. A feasible prototype model was built to convey the concept and to enable cost estimation. The SpaceX Falcon Heavy rocket with a 26,700 kg payload to GEO was selected to take the 675 tonne spacecraft into orbit; space station construction will require up to 30 launches, this would be reduced to 5 launches when the SpaceX BFR becomes available. The estimated total cost of implementing the Sussex Biocompatible International Space Station (BISS) is approximately $47.039 billion, which is very attractive when compared to the cost of the International Space Station, which cost $150 billion.

Keywords**—**Artificial gravity, biocompatible, geostationary orbit, space station.

I. Introduction

THE deployment of an International Space Station (ISS) into GEO is a relatively unexplored concept. The current ISS resides in a Low Earth Orbit (LEO) between 330 and 435 km, in comparison, GEO lies 35,786 kilometers above the Earth's equator and is currently used for communication and weather satellites. Objects in GEO follow the same orbital period as the Earth's rotational period meaning satellite antennas on Earth do not have to move to track a satellite making it favorable for communication and GPS. An ISS positioned in GEO would be advantageous to space travel and microgravity experiments. It would provide a docking station for spacecraft on long distance missions to refuel and restock, allow experiments to be conducted in variable and controllable microgravity environments and provide a platform for space tourism. The history of space travel is well documented in [1] and [2], and many more articles, providing detail of how space exploration began and evolved. All planets in the solar system have been visited by interplanetary space probes; however manned spaceflight has focused on establishing a permanent human presence in space through the development of Mir and the ISS, as observed in [3].

A summarized overview of the ISS is documented in [3]; it is noted as representing the largest scientific and technological cooperative program in history. The station resides at LEO between 330 and 435 km from the equator at an orbital speed of 7.67 km/s and an orbital period of 92.65 minutes [4]. Since the launch of its first module, Zarya, in 1988 more than 40 assembly flights have formed a station of approximately 1,000 cubic meters of pressurized volume, 400,000 kilograms of mass with approximately 100 kilowatts of power output. The 15 pressurized modules have been continuously occupied for over 16 years and serve as a research laboratory for the space environment. An important focus of the research is to explore the effects of microgravity and radiation on human health. Understanding the use of the current ISS helps to show the potential advantages of the station proposed in this project.

There are endless risks associated with space travel; the most predominant being space debris, radiation and zero gravity. Space radiation originates predominately from three natural sources; Solar Particle Events (SPE), Galactic Cosmic Radiation (GCR), and trapped radiation, all of which provide serious potential hazards for space operations such as cancer, circulatory diseases and cataracts [5]. There has been a number of published papers on the hazards of space travel, [6] states that the ISS is thought to be exposed to an approximate 200 mSv of radiation, over 80 times the amount experienced on earth and double the level for which cancer is more likely. Reference [7] estimates that approximately 30% of the cells in the body will be affected by ionizing events on a three-year interplanetary trip. The effect of space radiation on the immune system is one that has not been extensively studied, it is estimated that the probability of the immune system being affected is equal to or even greater than the probability of inducing mutations [8].

The ISS has been designed to reduce radiation exposure using shielding and up-to-date weather alerts including geomagnetic field conditions, solar cycle position, and interplanetary proton flux, [9] these alerts allow the astronauts to move to more protected areas of the spacecraft when required. Reference [10] outlines the general dynamics and engineering design associated with spacecraft system shielding, the publication documents operational spacecraft environments and how they can be protected. There has been considerable research undertaken into the effects of zero gravity. Reference [11] states that 'prolonged exposure of humans to a weightlessness environment can lead to significant loss of bone and muscle mass, cardiovascular and sensory-motor deconditioning'. Maintenance of bones requires high-force impulse loading coupled with a continuously applied load along the axis. Absence of this, as there is in

Chris. R. Chatwin is a Professor in Engineering at the University of Sussex, Dept. of Engineering, Brighton BN1 9QT, UK (corresponding author, phone: +44 1273 678901; e-mail: C.R.Chatwin@sussex.ac.uk).

Tim Falk is an Engineer in the Department of Engineering, University of Sussex, Brighton BN1 9QT, UK (e-mail: tjf24@sussex.ac.uk).

microgravity, causes the bones to deteriorate resulting in a decrease of the net amount of body calcium.

Cardiovascular deconditioning is also a response to microgravity; [12] highlights a number of studies into the debilitating effects on the cardiovascular system in space in the presence of zero gravity. Sensory-motor deconditioning associated with microgravity causes changes within the vestibular and somatosensory systems that can affect the control of posture and movement [13]. It is concluded in [14] that about 90% of astronauts suffer from 'mal de debarquement syndrome', an imbalance sensation, following long-duration missions. The previously stated are just a few of the known physiological effects of zero gravity, thus making artificial gravity is an essential requirement for future spaceflights.

Artificial gravity is created using centripetal acceleration [15]. 'Deliberate architectural design for the unusual conditions of artificial gravity will aid human adaptation to space and improve the habitability of the environment.' [16] Ideally the centripetal acceleration produced is of a magnitude of 1g, Earth's gravity. However, a number of authors [12], [14] have stated that considerably lower values are beneficial. Experiments performed on the degree of comfort in artificial gravity are well documented in [17]. Although some conclusions differ, a general comfort zone between 0.3-1g was established. Angular velocity also requires careful consideration as a high value can lead to dizziness, motion sickness and the Coriolis Effect. It is observed in [18] that higher rpm led to a higher susceptibility to motion sickness, with a degree of adaptation required, a conclusion gained from conducting a number of experiments within a 15 ft rotating room. In contrast, [19] noted that sensory-motion adaption to 10 rpm can be achieved if the subject makes the same movement repeatedly. This repetitive movement allows the nervous system to gauge and adapt to how the Coriolis forces generated as the movements within the rotating reference frame are deflecting movement paths and endpoints.

Details of how the ISS is protected from meteoroids and orbital debris are outlined in [20]. It explains how the space station's risk management has developed a strategy to mitigate the meteoroid and debris hazard involving shielding, collision avoidance, and damage control. The primary debris environment model was implemented in 1991 [21] and consisted of a flux and velocity model. Since then the model has been updated and is primarily used to assess whether elements of the ISS meet their Probability of Penetration (PNP) specification. PNP calculates the number of potential collisions resulting in hull penetration over a 10-year period, an overall minimum value of 0.81 is implemented for the entire space station with vital compartments having higher values and less important compartments lower values.

Over 100 different shields have been designed, tested and are currently implemented onto the ISS, the most common and effective being the Whipple bumper. The Whipple bumper is most effective at high impact velocities as it disperses the objects energy at a distance away from the pressure hull [22]. Reducing the risk of space debris impact not only serves as protection for the astronauts but also serves to minimize the amount of debris within the orbit. The Inter-Agency Space Debris Coordination Committee (IADC) established space debris mitigation guidelines with the fundamental principles of limiting the amount of debris and minimizing the potential for on-orbit breakups, post-mission disposal and prevention of on-orbit collisions [23]. The fundamental principles of spacecraft structures, designs, assembly's and manufacturing materials are provided in [24]. In [24] it is stated that there are currently considerable bodies of advanced technology available and in development at NASA that could provide additional substantial improvement to spacecraft if development is successfully completed.

The objective of this article is to present generation of cost effective BISS that provides a biocompatible environment that will protect astronauts from radiation, space debris and the health hazards insipient in a microgravity environment. Recent advances in low cost launch vehicles make this an affordable and realistic possibility.

II. Hazards of Space Exploration

Space is one of the most extreme environments known to man with endless physical, biological, psychological and sociological hazards to be contained. This section covers the main risks associated with space travel and how the space station will mitigate these risks.

A. Space Debris Hazard

Due to increased space activity the earth is now surrounded by a vast population of satellites located in all orbital zones each with a diversity of tasks. Impacts with natural bodies, such as meteorites, collisions between spacecraft and re-entry or breakup events of satellites at the end of a satellite's lifetime all greatly contribute to produce swarms of new orbiting objects. The Kessler syndrome, proposed by NASA scientist Donald J. Kessler in 1978, describes a self-sustaining cascading collision of space debris. The scenario states each collision generates more objects that increase the likelihood of further collisions [25]. The proliferation of this swarm of space debris represents a serious threat to current and future missions [26]. The United States Strategic Command department stated that as of July 2013 more than 170 million debris smaller than 1 cm, 670,000 debris between 1-10 cm and 29,000 larger debris were estimated to be in orbit, each as deadly as the next [27]. A collision with a 1 cm object would likely disable and penetrate the ISS shields, a collision of a typical satellite with an energy-to-mass ratio exceeding 40 J/g is considered catastrophic [25].

Higher altitudes, such as GEO, are used less commonly and thus have a lower population of debris. Close approaches, within 50 meters, are estimated to occur at least once per year. The NASA Orbital Debris Observatory (NODO) along with the US Strategic Command (USSC) tracks and documents orbital objects as small as 1 cm to ensure satellites and manned stations remain clear of the debris. However, since GEO is too distant to accurately measure objects under 1 m, the degree of the space debris problem is unknown.

In an attempt to deal with the debris in orbit around the Earth, the IADC, an international intergovernmental forum, was founded in 1993. The fundamental principles of the forum are: limitation of debris released during normal operations, minimization of the potential for on-orbit break-ups, post-mission disposal, and prevention of on-orbit collisions [23]. Mitigation measures have been established to limit the debris risk on missions and launches.

To remain in compliance with the IADC, the proposed space station will incorporate a propulsion system that is unable to be separated from the spacecraft. In the case that requires separation, the propulsion system is designed to remain in an unpopulated orbit outside of the protected geosynchronous region known as the graveyard orbit. This orbit lies away from common, highly populated areas - typically a super-synchronous orbit at a considerable distance above synchronous orbit [28]. Whilst efforts from associations such as the IADC and NODO minimize the hazards of space debris, the issue arises not only from manufactured junk but also from natural phenomena such as meteoroids and asteroids. Impacts from high-velocity debris have the potential to cause spallation, perforation, shocks, temperature and pressure changes, and crack growth phenomena, all of which can be detrimental to the astronaut's health.

The space station will incorporate damage control, shielding, and collision avoidance to reduce the risk of substantial damage. Damage control is to be similar to that of the ISS risk management strategy where PNP values are specified on elements of the station. Compartments with lower PNPs are required to be further reinforced than those with higher values. The ISS's overall PNP requirement is 0.81, equivalent to a 0.2 probability that one or more penetrations of a critical item will occur over a 10-year period. A PNP of 0.8 would expect 0.21 critical penetrations (N_p) over a 10-year period, calculated using (1) [20]:

$$N_p = -log_e(PNP) \quad (1)$$

State-of-the-art shielding is also to be manufactured for the BISS. Whipple shields are a type of spaced, hypervelocity impact shield capable of protecting against velocities ranging from 3-18 km/s. The shield is based upon the principle that miniature meteoroids explode when they collide with a solid surface, thus removing the energy of the meteoroid and spreading the slowed projectiles over a larger area of the next layer, the catcher. The simplest form of the shield consists of a thin sheet of aluminum, called the bumper, that is positioned a small distance away from the next layer of the catcher. This distance acts as a buffer allowing remaining fragments that puncture the bumper to disperse preventing any essential layers such as the pressure layer from being penetrated [29].

Stuffed Whipple shields incorporate layers of Kevlar and Nextel inserted between the bumper and the catcher, preventing further shock and pulverizing the debris cloud ensuring that any fragments that reach the catcher layer are harmless, this is to be used on the more vital modules of the station. A more common design is the multi-shock shield; this consists of staggering layers of Nextel at specific standoff distances. This repeatedly shocks the projectile and debris cloud removing all energy from the fragments preventing them from breaching the rear wall [29]. Fig. 1 [20] represents the layouts of potential shielding configurations showing spacing between each stage of the shield as well as plate material and thickness.

Manufacturing the proposed space station with appropriately positioned Whipple shields, continuation of monitoring orbiting debris as a way of collision avoidance and strict damage control will thoroughly reduce the risks from space debris.

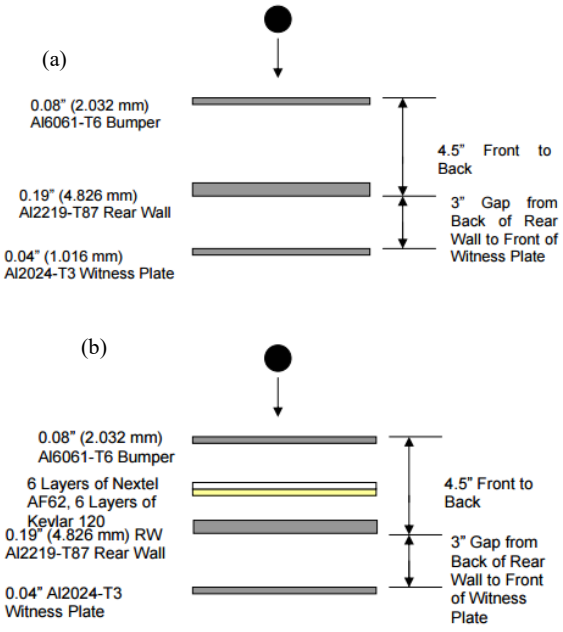

Fig. 1 (a) Whipple shield configuration, (b) Enhanced Stuffed Whipple shield configuration

B. Radiation Hazard

Radiation is energy that is emitted in the form of high-speed particles or electromagnetic waves [30]. Radiation may have sufficient energy to cause ionization in the medium through which is passes [31]. Space radiation is naturally sourced from: SPE, GCR, and trapped particle belts such as the Van Allen belts. The Van Allen belts represent two magnetic rings surrounding the Earth containing trapped particles due to the Earth's magnetic field. The outer belt extends to 37,300 miles; GEO is situated within this at an altitude of 22,300 miles [32]. A fluctuating population of high-energy electrons ranging from 0.1-10 MeV is present; however, more severe radiation is located at lower altitudes. GCR originates outside the solar system and consists of ionized atoms, predominately protons, ranging from a uranium nucleus to a single proton. Exposure to these particles increases at higher altitudes, they have a higher energy than trapped particles making them difficult to shield against at GEO.

SPE are the occurrence of high energy particle flux, mainly energetic protons, over a period with an energy greater than 10

MeV [33]. The particles are accelerated to a fraction of the speed of light by interplanetary shock waves that exist near solar flare sites. The highly energized particles temporarily enhance the radiation dosage around the magnetosphere in interplanetary space.

The threat to human health from exposure to ionizing radiation poses a significant challenge; ionizing radiation has a deleterious effect on human tissue [34], which can be divided into two categories: deterministic and stochastic. Deterministic effects are caused by death or significant damage to cells. Physical effects, such as radiation sickness and sterility, occur when the magnitude of cell deaths is large enough to cause functional impairment of organs or tissue. The severity of the effects is related to the magnitude of dose and will only occur once a threshold of exposure has been exceeded. Stochastic effects are caused when damage to a cell's DNA has caused it to break and re-join incorrectly or it has re-joined as a symmetrical translocation with the potential of an oncogene gene occurring during division; this can lead to cancer or hereditary defects. The latent periods of deterministic and stochastic types are 2-4 week and 10-20 years respectively [8] indicating there are both long and short term effects of exposure.

May 8th 2003 saw the launch of GSAT-2, an experimental communication satellite built by the Indian Space Research Organization, containing a Total Radiation Dose Monitor (TRDM) within its payload. Once in orbit it conducted a number of experiments to compare the directly measured radiation dose at GEO with an estimated radiation dose inside the satellite using a Radiation Sensitive Field Effect Transistor (RADFET) [35]. The objective of their experiment was to measure accumulated dose at the center of spherical aluminum shields of different thickness and to compare the values with the dose derived from NASA models. Table I represents the dose results obtained over an approximate 480-day period [35]. As expected, the thicker the shielding the lower the dose experienced. Dividing the total dose by the number of days and converting it to SI units mSv shows that the average daily dose γ_{ave} experienced is approximately 967 mSv, as shown by (2):

$$\gamma_{ave} = \frac{46430}{480} \cdot 10 = 967.29\ mSv \quad (2)$$

TABLE I
ACCUMULATED DOSE MEASURED BY TRDM

Dosimeter (Dome Thickness)	GTO Dose (rads/ 2days)	Total Dose (rads)	GSO Dose (rads/ year)	Dose Rate (rads/ min)	Oct. 2003 Solar Flare Dose (rads)
GRD-10 (0.8 mm)	4430	46430	42130	0.08	2790
GRD-20 (2.8 mm)	378	1912	1534	0.0029	256
GRD-30 (5.74 mm)	27	403	376	0.00072	60
GRD-40 (8.86 mm)	13	394	381	0.00072	60

Exposure to a 1,000 mSv dose gives roughly 1 in 20 chance of developing cancer, in perspective; the average exposure experienced per year on the ISS is 150 mSv and on Earth 3.01 mSv. Radiation not only poses a severe risk to human health but also to the semiconductor electronic components on-board the space station. Charged particles can cause electronic noise, signal spikes and can knock electrons loose within the systems. To overcome this issue, radiation hardening is implemented on all susceptible devices. Radiation hardening is the act of increasing an electronic component's and system's resistance to damage or malfunctions caused by ionizing radiation.

An estimated 95% of radiation irradiating the ISS is blocked through a combination of shielding and internal radiation monitoring. Following similar methods implemented on the ISS along with innovative ways of shielding from radiation, the proposed BISS will achieve an enhanced percentage of shielding. A number of parameters are to be implemented to reduce exposure, as detailed in the next section.

Fig. 2 represents one of the eight accommodation modules positioned in a ring configuration connected by curved walkways. Each module has its own solar array that is positioned to face normal to the sun's rays, thus acting as a shield protecting against the worst of the sun's rays. The multi junction solar cells consist of stacked Indium Gallium Arsenide (InGaAs) that has been proven to have superior radiation-resistance.

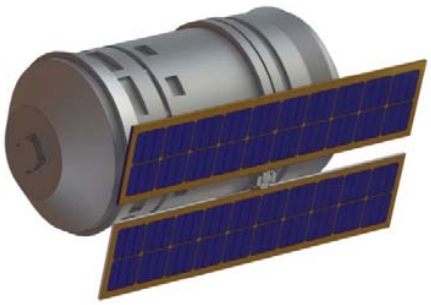

Fig. 2 Accommodation module and solar panel render

There has been considerable research and development into manufacturing materials that are able to effectively block radiation particles. A study conducted by NASA in 2002 determined that materials with a high hydrogen content, such as polyethylene, could reduce primary and secondary radiation to greater extents than commonly used metals such as aluminum. High hydrogen content materials such as plastics are effective as they produce far less secondary radiation than heavier materials due to hydrogen having the highest charge-to-mass ratio of any element. Secondary radiation originates when charged particles strike the atoms within the shield triggering nuclear reactions causing a shower of neutrons and other particles to enter the spacecraft [36]. Hydrogen is considered the most effective shielding material as it is effective at stopping protons that are found in solar particle emission events, splitting heavy ions that are found in GCR, and slowing down neutrons that are formed as secondary radiation when the GCE and SPE interact with matter. However, hydrogen itself is not a solid material and currently

available materials such as polyethylene that contain a lot of hydrogen do not possess sufficient strength for spacecraft applications. This is one of the key reasons why aluminum is so widely used.

There are a number of prototype materials in development such as polyethylene RXF1 that has been found to be 50% better at blocking solar flares and 15% better for cosmic rays in comparison to aluminum, as well as having 3 times the tensile strength and being 2.6 times lighter. Hydrogenated Boron Nitride Nanotube (BNNT) is also a promising material in development, due to its high levels of boron and hydrogen it is effective at capturing harmful neutrons. It too has a high content of hydrogen and has been experimentally proven effective at shielding GCR and SPE doses, as shown in Fig. 3 [37].

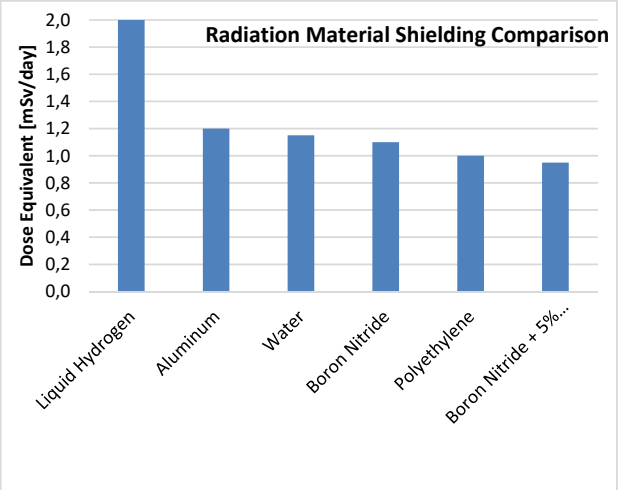

Fig. 3 Calculated exposure to GCR with shielding by a wall of the same thickness (30 cm) made of various materials

Fig. 3 shows a comparison of how effective a variation of materials, each with a thickness of 30 cm, are at shielding radiation, any dose below 1.0 mSv is considered state-of-the-art. BN+5% is shown to perform the best due to its molecular nanotube structure, high density and high hydrogen content. Suitable materials are also required to have high strength and temperature stability whilst being affordable and lightweight. The structural material properties of BNNT greatly exceed those in current use due to its high young's modulus of almost 1000 GPa. Despite these developments in radiation shielding, these materials are still in development and not currently in practical use and thus cannot be used for this project. Therefore, the conventional use of aluminum is to be primarily used as it provides shielding and sufficient structural strength.

There are a number of techniques that can be employed when manufacturing the spacecraft such as storing water within the walls and using polyethylene multilayer insulators as both are readily available, lightweight and effective at shielding from radiation. Naturally, a thicker material provides greater protection; however, thickness greatly increases weight that increases launch costs. Fig. 4 shows the effect that thickness has on shielding effectiveness for aluminum and polyethylene shields [38].

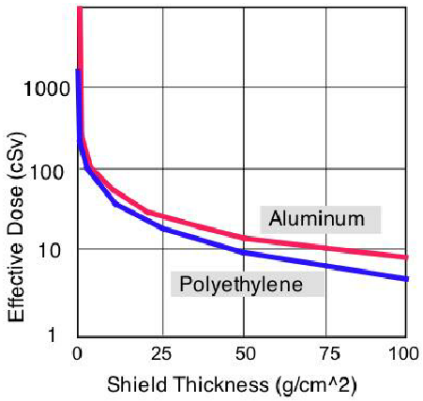

Fig. 4 Radiation dosage to material thickness graph

A combination of shielding and insulating materials is currently used in a number of active spacecraft. Multilayer insulation (MLI) is composed of multiple thin layers of a variety of materials primarily intended as radiation heat transfer barriers to block the flow of radiative and thermal energy, they are capable of blocking up to 99% of radiation it is exposed to. The insulator consists of a number of synthetic polymers such as polyethylene and silicone as well as reflective layers and radiant barriers that inhibit heat transfer by thermal radiation. The low emittance of the surface prevents radiation from transferring thermal energy from one side of the insulator to the other [39]. Additional layers can be added to the MLI to reduce loss further, the performance of the insulator can be defined by the radiative heat flow rate *(q)* between two parallel surfaces as shown in (3) [30]:

$$q = UA\Delta T \tag{3}$$

where U is the heat transfer coefficient, A is the cross sectional area and ΔT is the temperature difference.

The Space Radiation Analysis Group (SRAG) at the NASA Johnson Space Centre is responsible for ensuring that the astronaut's exposure to radiation remains below established safety limits. The National Oceanic and Atmospheric Administration (NOAA) relays data and alerts to the SRAG received from ground stations and space weather satellites; this ensures that the astronauts are moved to safer locations within the spacecraft if a solar event or peak in radiation were to occur. SRAG maintains an extensive set of equipment for measuring the exposure received by the astronauts; these tools include trajectory translator/propagator algorithms, time-resolved models of the Earth's magnetic field, and maps of radiation fluxes trapped in the geomagnetosphere. Radiation dosage monitoring instruments are also provided to quantify the environment outside [40] and inside the spacecraft [41].

C. Microgravity Hazard

Microgravity is known to be one of the greatest hazards associated with space with potentially detrimental

physiological, psychological and sociological effects to the human body and mind. Equation (4) [41] represents universal law of gravitation, the attractive force between any two bodies:

$$F_g = G_u \frac{Mm}{d^2} \quad (4)$$

where m and M are the masses of an object and the earth respectively, d is the distance between their centres of mass and G_u is the universal gravitation constant, 6.67408×10^{-11} $m^3 kg^{-1} s^{-2}$. Equation (5) [41] gives the force experienced of any mass at the surface of the Earth:

$$a = G_u \frac{M}{d^2} \quad (5)$$

Inserting the Earths radius of 6,371 km and mass of 5.972 x 10^{24} kg into (5) gives an acceleration of approximately 9.81 m/s^2. The gravitation pull at GEO can be calculated by substituting in the resulting orbital radius of GEO including Earths radius, 42,164 km. This gives an acceleration of 0.224 m/s^2 thus it is referred to as microgravity and not zero gravity; however, the acceleration is so minimal that it is not felt nor does it noticeably affect objects within its vicinity. Humans have spent possibly 10^5 years evolving and adapting to the effect of gravity, extended periods of exposure to microgravity has proven to have deleterious effects on human biology. Short-term exposure commonly causes what is known as space adaptation syndrome in which space travelers experience motion sickness as the vestibular system adapts to weightlessness [42]. Long-term exposure causes multiple health problems, the most significant being loss of muscle and bone mass.

With the absence of gravity, skeletal muscles are no longer required to maintain posture and the main muscle groups are no longer required for movement causing bone and muscle deterioration. Without regular exercise astronauts can lose up to 20% of their muscle mass in 5-11 days. Bone tissue can deteriorate at a rate of up to 1.5% a month as well as rapid bone loss from 3% per decade to approximately 1% per month due to the decreased axial load on bones [43]. This rapid decrease in bone density causes brittle bones resulting in symptoms similar to those of osteoporosis. 3-4 months in space can take 2-3 years to regain lost bone density due to osteoblasts, cells that make bone, not being consecutively active [44]. In an attempt to prevent these effects the ISS is equipped with a number of exercise machines such as treadmills, weight machines and resistive exercise devices all of which are adapted to be used in zero gravity conditions. Astronauts are required to spend at least two hours per day exercising [45].

The human body consists of 60% water, as soon as it is exposed to microgravity, fluid is re-distributed to the upper body resulting in a puffy face, bulging neck veins, and sinus and nasal congestion, this is visually represented by Fig. 5 [44]. Astronauts can lose up to 22% of their fluid blood volume, this reduction in blood can cause the heart to atrophy and thus decrease in size, strength and activity. Senses can also be greatly disrupted such as vision, taste and intracranial pressure due to prolonged periods of microgravity. Asthenization is a condition experienced by astronauts following return to earth after a long-term space flight; symptoms include: fatigue, irritability, lack of appetite, and sleep disorders.

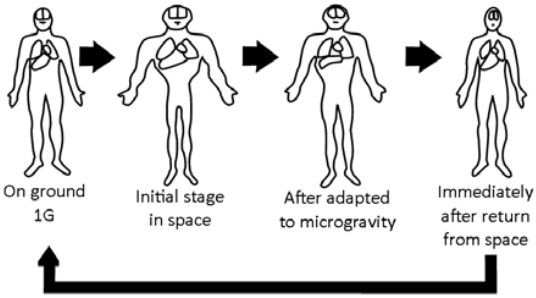

Fig. 5 Effects of microgravity on fluid distribution, greatly exaggerated

Psychological and sociological effects of spaceflight are commonly experienced after long-term missions. The amount of sleep experienced in space is poor due to highly variable light and dark cycles, poor illumination during daytime and the effect of microgravity. Disturbances in circadian rhythm can have profound effects on neurobehavioral responses of the crew and aggravate the psychological stresses they experience. High workloads and increased sound levels also reduce the amount of sleep, approximately 50% of astronauts get 2 hours less sleep each night than they would do on earth, many of them are forced to take sleeping pills [44]. Lack of sleep and isolation with the same small group of people for long periods causes considerable stress that can cause disagreements within the team. There have been many advancements in space medicine to attempt to reduce the physiological, psychological and sociological effects associated with space travel such as hormone supplements to help maintain muscle and body mass. This BISS should remove these effects entirely by creating artificial gravity.

III. Artificial Gravity

The notion of simulating gravity through centrifugation was introduced early in the conception of human space travel. The idea of a rotating wheel-like space station dates back to the writings of Tsiolkovsky, Noordun and Wernher von Braun [10].

A. Comfort Parameters

There has been considerable literature and experimental data undertaken in an effort to determine comfort criteria [15], [17] for rotating spaceships. Much of this research has taken place in rotating simulators or centrifuges at the NASA Langley Research Centre. Several authors have published guidelines for criteria; Table II represents a summary of their findings [46]. Assuming the environments rotation is constant, artificial gravity depends on the quantities explained below.

TABLE II
COMFORT BOUNDARIES IN ARTIFICIAL GRAVITY

Author	Year	Radii [m] min. r	Angular Velocity [rpm] max. ω	Tangent Velocity [m/s] min. V_t	Centripetal Acceleration [g] min. a_c	Centripetal Acceleration [g] max. a_c
Hill & Schnitzer [46]	1962	-	4	6	0.035	1.0
Gilruth [46]	1969	12	6	-	0.3	0.9
Gordon & Gervais [46]	1969	12	6	7	0.2	1.0
Stone [46]	1973	4	6	10	0.2	1.0
Cramer [46]	1985	-	3	7	0.1	1.0

Circular motion is characterized by a radius, r and an angular velocity, ω, the radius is measured from the center of gravity of the rotating environment. Centripetal acceleration (a_c) is directly proportional to the radius thus maximizing the radius reduces gravitational gradient, the difference in artificial gravity level with distance from the center of rotation. A minimum radius of 12 m was specified which gives an approximate gravity gradient of 15%, as shown in Fig. 6 [46]. This limit takes into account human factors that affect the work efficiency, for example, an object will get heavier the closer to the edge of the rim it gets.

The angular velocity of a rotating body is defined as the rate of change of angular displacement, and is a vector quantity that specifies the angular speed of an object and the axis about which the object is rotating. The cross coupling of normal head rotations inside the rotating room can lead to motion sickness and dizziness; to minimize this the habitats angular velocity must be minimized. A maximum angular velocity of 2 rpm was assigned as the comfort criteria for this parameter that takes into account the comfort literature and the objective to make the spacecraft as habitable as possible. For a circular path, (6) [46] defines angular velocity:

$$\omega = \frac{v_t}{r} \tag{6}$$

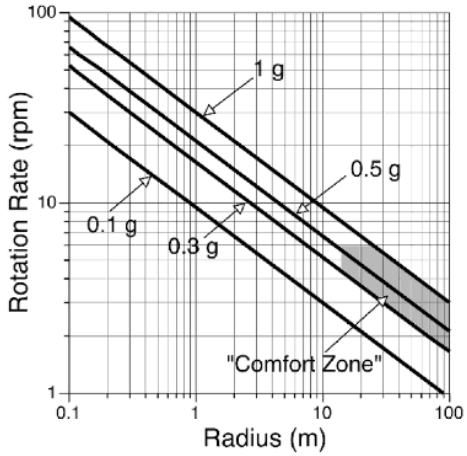

Fig. 6 Rotation rate as a function of radius for four gravity levels

Tangential velocity describes the motion along the edge of a circle; the direction at any given point on the circle is always along the tangent line, as shown by Fig. 7.

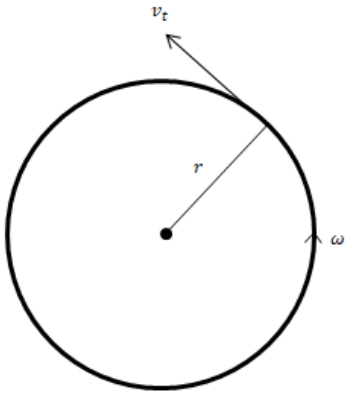

Fig. 7 Tangential Velocity, v_t

Objects moving within a rotating habitat are subject to Coriolis acceleration that distorts the apparent simulated gravity. For relative motion in the plane of rotation, the ratio of centripetal to Coriolis acceleration is twice the ratio of the subject's tangential velocity to the relative velocity. To minimize the Coriolis Effect and velocity ratio, the tangential velocity is required to be maximized. A minimum tangential velocity of 10 m/s was assigned as this value complies with the comfort criteria. The tangential velocity of any point is proportional to its distance from the axis of rotation and rotation, thus re-arranging (6) [46]:

$$v_t = \omega r \tag{7}$$

Centripetal acceleration is the acceleration of an object relative to its environment. The level of centripetal acceleration defines the force that is experienced by an object on the rim of the spinning spacecraft, thus is the level of artificial gravity. A body that moves in a circular motion of radius, r, at a constant speed, v, is always being accelerated, the acceleration is at a right angle to the direction of rotation, towards the center of mass.

The direction of acceleration is deduced by symmetry arguments, the directions of the velocity vectors are shown in Fig. 8 [47]. Equation (8) gives the magnitude of acceleration:

$$a_c = \frac{{v_t}^2}{r} = \frac{(\omega r)^2}{r} = r\omega^2 \tag{8}$$

A minimum magnitude of acceleration of 3.711 m/s^2 is assigned to BISS; this is the gravitational acceleration for Mars, which is a substantial enough to mitigate the deleterious

effects caused by microgravity. To specify Earth's gravitational acceleration of 9.81 m/s^2 would make the BISS far too expensive.

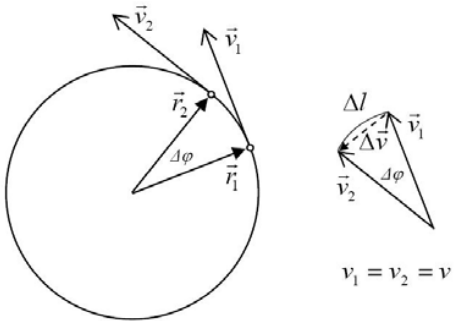

Fig. 8 Direction of centripetal acceleration

The Coriolis Effect is the apparent deflections of the path of an object moving within a rotating coordinate system. Coriolis acceleration is proportional to the vector product of the objects' relative velocity and the environment's angular velocity, acceleration is zero when the relative velocity is parallel to the axis of rotation. The Coriolis Effect will be greater the closer the object moves toward the center of rotation, therefore to reduce this effect a larger diameter is required. Coriolis force remains constant regardless of the distance from the center of rotation, the direction of these forces are shown in Fig. 9 [46]. The direction of this force is perpendicular to the plane formed by the angular velocity. Equations (9) and (10) define the magnitude of the force and acceleration respectively.

$$F_c = 2m\omega v \tag{9}$$

$$a_{cor} = 2\omega v \tag{10}$$

Although reducing the angular velocity decreases the likelihood of motion sickness and dizziness, due to the radius of the space station being limited because of economic implications, other aspects of gravitational distortion may increase. The ratio of the magnitude of centripetal acceleration and the magnitude of the Coriolis Effect is one measure of this distortion [16]. Simulating a natural gravitational environment requires this ratio to be minimized without constraining the relative motion of people or objects within the environment. This ratio is represented by dividing the Coriolis acceleration, (10), by the centripetal acceleration, (8), as shown by (11) [46].

$$\frac{a_{cor}}{a_c} = \frac{2\omega v}{r\omega^2} = \frac{2v}{r\omega} \tag{11}$$

Once a maximum feasible radius is reached a further reduction of angular velocity, ω, decreases both the Coriolis and centripetal accelerations whilst increasing the ratio of Coriolis to centripetal. Thus whilst reducing ω, ameliorates problems associated with rotational cross-coupling it exacerbates gravitational distortion and the Coriolis effect.

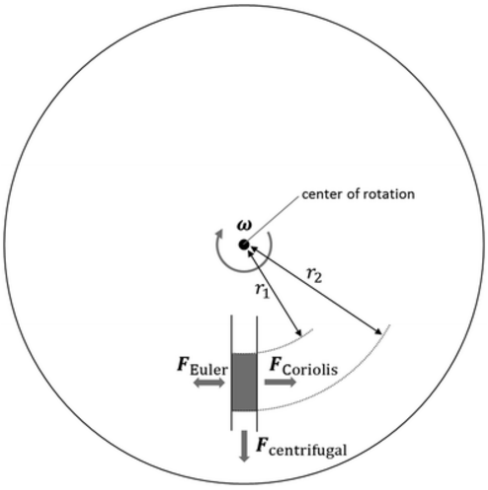

Fig. 9 Pseudo-forces acting in a centrifuge

The comfort parameters detailed above allowed the smallest possible radius of the space station to be calculated. Values for centripetal acceleration and angular velocity were assigned as 3.711 m/s^2 and 2 rpm respectively (12).

$$\omega = 2 \cdot \frac{2\pi}{60} = 0.209 \left(\frac{rad}{s}\right) \tag{12}$$

Equation (8) is then re-arranged for radius to be the subject, as shown in (13):

$$r = \frac{a_c}{\omega^2} = \frac{3.711}{0.209^2} = 84.957m \cong 85m \tag{13}$$

The tangential velocity was calculated using (7):

$$v_t = r\omega = 85 \cdot 0.209 = 17.765 \frac{m}{s} \tag{14}$$

Therefore, the four parameters that characterize the artificial-gravity environment are defined as follows:

- Radius, r: from centre of rotation = 85 m
- Angular Velocity, ω: spin rate = 2 rpm
- Tangential Velocity, v_t : rim speed = 17.765 m/s
- Centripetal Acceleration, a_c: gravity level = 3.711 m/s^2

IV. Space Station Design

The main objective of this space station design is to create a safe, habitable environment that can remove or diminish the hazards associated with space travel. Achieving this would provide a number of potential uses for the station such as space tourism, experiments and a docking station for spacecraft on long-haul missions. The prototype design of the space station is displayed in Fig. 10; Fig. 16, in the appendix provides some dimensional data. The station is comprised of eight pressurized modules, eight solar truss arrays, eight connecting walkways, and four support beams that connect the modules to the central docking module. This section analyses the mechanical structure of the space station, covers general living amenities, and details how the station will remain in

GEO.

Fig. 10 Model of the Biocompatible Space Station – produced using SolidWorks®

If successful, this space station will be the largest structure ever to be built in space. A full structural analysis is vital to determine the effects of the loads on the physical structures and their components. Due to the space station being situated in GEO it will experience microgravity and thus will encounter minimal external forces acting upon it. The main stresses will occur from the rotation of the ship due to centrifugal forces in which inertia force is directed away from the axis of rotation toward the rim. The magnitude of the force F applied can be defined by Newton's law of motion, which states that the rate of change of momentum of a body of mass m is directly proportional to the force and direction applied, as shown by (15):

$$F = ma \tag{15}$$

Any motion in a curved path represents accelerated motion and requires a force directed toward the center of curvature of the path. Substituting (8) into (15) for acceleration a gives (16) [41], the equation for centripetal force:

$$F_c = m\frac{{v_t}^2}{r} \tag{16}$$

Equation (16) defines centripetal force to be proportional to the square of the tangential velocity, indicating that doubling the speed produces four times the centrifugal force. The mass of each module was calculated by multiplying the volume evaluated from the SolidWorks® 3D model, by the density of aluminum 2219-T6, 2.84 g/cm^3, from which it is manufactured. The maximum stresses on each component are shown in Table III.

A number of simulations were carried out in SolidWorks® on a simplified version of the space station in order to test the deflection and stress experienced by the structure of the spacecraft thus ensuring that it is sufficiently strong. Fig. 11 shows the deflection simulation result; as shown, the majority of the deflection and stress is experienced by the connecting walkways as they are the thinnest sections and support the accommodation modules. There is also high stress on the lower supporting beams near to the central hub; this is because stress in a rotating structure is highest near the center. The highest recorded stress was 4.51 MPa, comparing this to the yield strength of aluminum 2219-T6 of 280MPa gives a factor of safety of 62.1.

TABLE III
MAGNITUDE AND TYPE OF LOADING EXPERIENCED BY EACH COMPONENT

Component	Type of Stress	Stress (MPa)
Accommodation Module	Normal	0.187
Supporting Beams	Tensile	1.45
Connecting walkways	Hoop	16.99

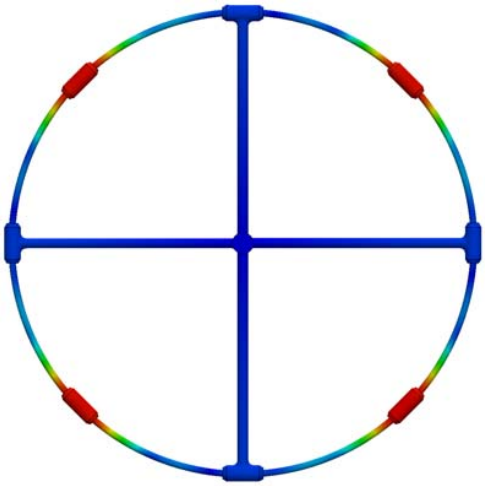

Fig. 11 Deflection Simulation Results

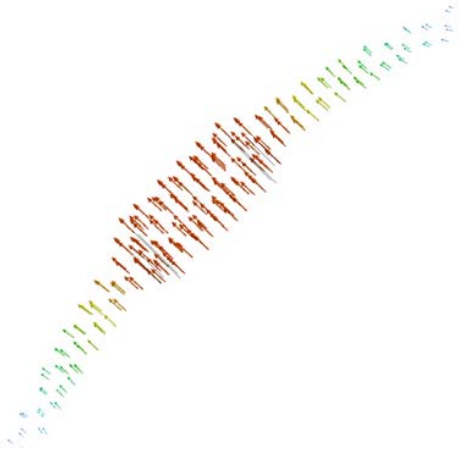

Fig. 12 Deflection of top left quadrant represented by vectors

Fig. 12 shows a quadrant of the vector deflection plot from the simulation. As shown, the majority of displacement occurred on the un-supported accommodation modules. This is because they do not have the support of the connecting

beams, thus despite experiencing the same magnitude of force as the other modules they experience a higher stress. The maximum-recorded deflection was 1.678 mm, the allowable elongation of 2219-T6 is 11%, thus the maximum allowable deflection for the thickness of the space station structure is 3.63 mm. This gives a factor of safety of 2.2, thus confirming that the structure is sufficiently stiff to deal with the applied load.

The space station is to be constructed of an appropriate mix of materials all of which are carefully selected for a specific function. The materials much resist, without failure or distortion, the static, dynamic, thermal and radiative stresses that the spacecraft will experience in service. These design requirements must be met with reliability and with a weight and cost limitation. The main structure of the spacecraft is to be manufactured out of 2219-T6 aluminum alloy due to its excellent strength-to-weight ratio and good fatigue strength, the T6 refers to the material being heat treated and then artificially aged which increases its strength. The truss is designed as a latticework structure that provides rigidity to the modules, the pressure hull and aspects of the Whipple shield are also to be manufactured out of 2219-T6 aluminum.

There is a MLI layer throughout the walls of the spacecraft to protect from excessive heating and cooling along with other forms of passive thermal control and active thermal control systems used to keep the spacecraft's occupants and equipment within an acceptable temperature range. MLI are made up of a number of layered materials including; Beta Cloth, Tedlar, Kapton, Teflon, Polyester, and Polyethylene. A number of these materials are aluminized, reinforced or coated and backed depending on their use. Together these form a high-performance insulator which uses multiple radiation-heat transfer barriers to retard the flow of energy, typically these reflectors can reflect 90 to 99% of radiation exposure [39]. A typical stacking arrangement including a 15 mm standoff space to the rear pressure hull is shown in Fig. 13 [48].

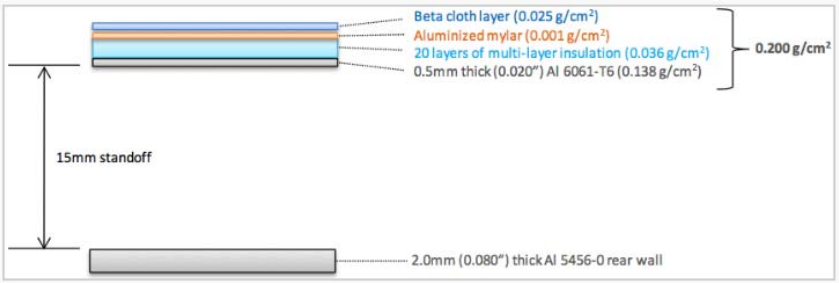

Fig. 13 Typical MLI Stacking Arrangement

The Whipple shield consists primarily of aluminum but can also feature protective materials such as Kevlar or Nextel aluminum oxide fiber in the case of stuffed Whipple shields. Exposed aluminum surfaces are to be anodized or coated in anti-corrosion paint to prevent atomic oxygen reactions and increase thermal efficiency. Interior structures and components are to be manufactured out of lightweight materials such as carbon fiber in order to save weight and decrease the payload of the rocket. Titanium and Stainless steel are used for plumbing, silicon insulation for wiring and Teflon for hoses. There are numerous other materials used for different applications around the spacecraft such as a Gallium Arsenide substrate within the solar panels.

Basic living amenities such as entertainment, food, beds, showers and toilets are naturally provided to create a comfortable environment for the astronauts. To save on weight and storage, specially created food is processed in sealed plastic bags, each bag has specific requirements to ensure that the astronauts have a balanced nutritional and vitamin diet. Calorie requirements differ between astronauts, for example, a large male requires about 3,200 calories a day whilst a small female requires about 1,900 a day [49]. Due to this station creating artificial gravity the need for specially altered food is reduced, condiments such as salt and pepper and other foods can be provided in their normal form.

The ISS features fan-driven vacuum toilets to deal with the absence of gravity, solid waste products are collected and stored and liquid waste evacuated. Showers are not featured on the ISS instead astronauts use wipes and a water-jet to wash. The addition of simulated gravity allows the use of conventional showers and toilets to be used creating a natural, homely living environment.

The electrical system is a critical resource for the space station as it allows the crew to safely operate the spacecraft, live comfortably and perform experiments. Power will be generated through a photovoltaic system, which converts light into electricity using semiconducting materials. The current solar arrays used on the ISS are single junction cells, which produce an approximate efficiency of 14% [50].

Photovoltaic cell technology has radically improved since the launch of the ISS with efficiencies reaching up to 46%. This is due to advances in multi-junction solar cells that have multiple p-n junctions consisting of different semiconducting materials. The different material junctions produce current in response to different wavelengths of light allowing a broader range of wavelengths to be absorbed. The materials for each layer are ordered with decreasing bandgaps thus allowing the light to transmit to the lower cell regions. The favorable material choice is InGaP for the top sub-cell, InGaAs for the middle cell and Germanium for the bottom cell. The triple-junction cells from Spectrolab are highly stable, producing approximately 2% additional power than predicted over a 3-

year period.

Multi-junction cells can be laminated between flexible sheets with metal foil circuitry resulting in a very small storage volume, up to 10 μm thick, and high specific power reducing the payload mass and thus the number of launches required [51]. The panels are to be mounted on solar tracker devices that orient the cells towards the sun to maximize absorption. Due to these advancements and successful testing; foldable, lightweight, highly efficient multi-junction solar cells are to be used on this spacecraft along with nickel-hydrogen batteries to store excess energy and provide continuous power during the eclipse section of the orbit.

Orbital station keeping involves using thrusters to execute orbital manoeuvres that are required to keep the spacecraft in its assigned orbit. Equation (5) shows that GEO experiences a small degree of lunar/gravitation perturbation, typically 0.85 degrees per year, thus a propellant of approximately 45 m/s a year orthogonal to the orbital plane much is to be applied. This is known as the North-South control. The East-West control is designed to keep the orbital period synchronous with earth's rotational period and keep eccentricity sufficiently small, the combination of these controls compensates for latitudinal and longitudinal variations respectively. Radiation pressures and solar wind also exert small forces causing small degrees of orbital drift. Hall-effect thrusters are currently widely used on commercial GEO communication satellites; thrusters such as the SMART-1 electric propulsion system have the ability to provide a variable range of discharge power, specific impulse and thrust of the following magnitudes [52].

- Discharge power: 0.46 - 1.19kW
- Specific impulse: 1,00 – 1,600s
- Thrust: 30 – 70 mN

Hall-effect thrusters are a type of ion thruster in which propulsion is produced by establishing an electric field perpendicular to an applied magnetic field, which electrostatically accelerates ions [53]. They are suitable for GEO spacecraft as they are a highly efficiency electric propulsion system, which can run off the stations' renewable electrical power source, thus far they have had a 100% success rate out of the 240 thrusters in commercial use. Hall-effect thrusters will be used on this spacecraft for not only orbital station keeping and orientation control but also to provide thrust for the rotation of the ship to create centrifugal force.

V. Cost Estimate

Space exploration is the most expensive venture undertaken by human kind. The astronomical costs come from a wide range of sources but predominately from launch costs, R&D and reoccurring engineering costs. Whilst there is a significant lack of data it is still important to make an estimate of the possible cost of building and deploying BISS. This section covers an approximate break down of the costs involved in an attempt to determine whether this space station is feasible in today's world.

Space transportation is generally viewed as the biggest obstacle to the growth of space commercialization and exploration, typically representing 25 – 70% of the total budget. Advances in rocketry have moved on significantly since the launch of the ISS, with larger, cheaper rockets able to take heavier payloads to more distant destinations. Table IV shows a comparison of potential launch systems [54].

TABLE IV
Cost Comparison of Orbital Launch Systems

Vehicle	Origin	Manufacturer	Mass to GEO (kg)	Launch Cost ($ million)	Launches
Falcon Heavy	United States	SpaceX	26,700	90	3
Vulcan Centaur Heavy	United States	United Launch Alliance	7,200	-	Planned July 2021
Vulcan	United States	United Launch Alliance	6,500	100	0
Delta IV Heavy	United States	United Launch Alliance	6,750	100	11
Long March CZ5	China	CALT	14,000	-	5

The rocket selected for transportation in this evaluation is Falcon Heavy by SpaceX; its capabilities are shown in Table IV. It has a potential GEO payload far superior to that of any other available shuttle. The volume and mass of each BISS component was evaluated using SolidWorks® 3D modelling, knowing the cost per kilogram of launch, the total mass of each module is summed in order to estimate an approximate total launch cost, this is shown in Table V,

The total mass is rounded to 675 tonnes in order to take into account additional, unconsidered mass. Division of the total mass by the payload of the Falcon Heavy rocket to GEO reveals that it will take ≈ 25 launches to get the entire space station into orbit. Taking into account the possibility of failed launches and the fact that each launch will not likely have an optimum payload, a more realistic number of launches will be 30, multiplying this by the cost per launch of $90 million gives a total launch cost of approximately $2.7 billion. We note that Space X are developing the BFR launch system, which is expected to be available in 5 years; using this rocket the number of launches would reduce to five. The space shuttle program for the ISS cost $450 million per launch, this accounted for approximately a third of the total cost per mission, taking into account other variables associated with launches such as; salaries, training and launch sites the total launch cost worked out to be $1.4 billion [36]. Considering these variables for each launch of Falcon Heavy gives an estimated cost per launch of $270 million, bringing the total launch cost for the project to $8.1 billion.

TABLE V
Total Approximate Mass of the Space Station

Component	Mass (kg)	Number of Modules	Total Mass (kg)
Main modules	22,009	8	176,075
Connecting walkways	22,734	8	181,872
Supporting Beams	37,180	4	148,720
Solar Array	11,124	8	88,992
Central Hub	58,789	1	58,789
		Total	654,448

Re-occurring engineering costs derived from the exotic nature of the technology involved with space exploration is the reason for such high manufacturing costs. Space stations are not mass-produced products thus the majority of its components are one-offs and are required to comply with tight tolerances. Specific material requirements must be satisfied, mineral ores refined and organic compounds purified all of which require extensive expenditure from planning, extraction, delivery and testing costs.

The objective of this project is to use technology and materials that are currently available today. Substantial research has already been conducted on space stations and GEO thus the research and development cost can be minimized. However, artificial gravity, despite having experimental data, has never been achieved in an active space station. The ISS budget for development was approximately $17.08 billion [55], which included numerous factors involved with the planning and execution of the space station. These factors include; design, research, testing, technology development, manufacturing scheduling and budget planning; hence, a realistic estimated budget for research and development of BISS is $12.766 billion.

The spacecraft structure and materials contribute comparatively little to the total cost of the vehicle. The main cost drivers are the composite multilayer heat shields, solar arrays, and the cost of fabrication and assembly, not the raw materials themselves. The cost of sourcing and assembling the aluminum structure of the spacecraft is approximated to be in the range of $1,800/kg to $3,800/ kg [56]. The total mass of the aluminum components is 544,204 kg thus giving a cost of $2.64 billion. Multi-junction solar arrays cost approximately $33,735.3/kg, which includes deployment testing, cell stack, wiring, connectors, panel substrate, panel hinges & boom, delay actuators, potentiometers and assembly [57]. The total mass of the solar array components is 88,992 kg giving a total cost of $3 billion. There is approximately 1607 m of multilayer insulator required on the spacecraft, at approximately $3191.5/m [39] this gives a cost of $5.13 million for the material and assembly. Therefore, the total cost of raw materials and assembly is approximately $6.156 billion.

NASA currently has 17,345 employees with wages ranging from $42,978 to $146,076 [58], giving an average wage of $92,295 costing $1.6 billion a year. The ISS was constructed over 17 years from 1998 to 2015, assuming this project will have a similar timeline and that half of all NASA employees are to be a part of the project gives a total personnel cost of $13.6 billion.

There are a number of additional costs associated with this project, maintenance being the most substantial. NASAs budget request for 2017 is $19.15 billion, $5.05 billion of that is for current space operations and ISS maintenance, a breakdown of which is shown in Fig. 14, due to the scale of BISS an annual maintenance budget of $6.38 billion will be required. Since the space station is going to be manned, it is required to be human-rated, a certification stating it is worthy of transporting humans. NASA outsources this to a private company as part of its Commercial Crew Development program; United Launch Alliance proposed a budget of $6.68 million for human rating of its Evolved Expendable Launch Vehicle through a Review of United States Human Space Flight Plans Committee. Further costs such as mission systems, rehearsals, security services, liquid hydrogen fuel, and orbital assembly (snap and seal technology) can add on a further $25.5 million. Thus, the total addition costs are approximately $6.417 billion.

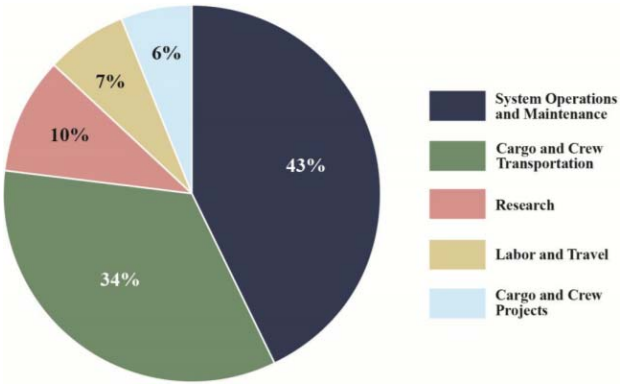

Fig. 14 Allocation of FY 2017 ISSs operating Costs

Table VI and Fig. 15 detail the estimated breakdown of the base costs involved with this project, the total overall costs are likely to be higher when expenditure on equipment and furnishings are taken into account. The cost is considerably lower than the cost of the ISS, $156 billion, for numerous reasons. Advancements in rocketry has significantly reduced the cost of launching to GEO and increased the magnitude of the payload meaning fewer trips are required for a smaller price. Another reason why the predicted cost is lower is due to new manufacturing techniques and composites materials, which allow for cheaper manufacturing of lighter, stronger components.

TABLE VI
ESTIMATED TOTAL COST OF THE SPACE STATION

Expenditure	Cost ($ billion)
Transportation	8.1
R & D	12.766
Materials	6.156
Personnel	13.6
Maintenance & Additional	6.417
Total	47.039

A large proportion of the ISS budget was on research and development, due to it being the first large-scale space station of its kind a lot of concepts had to be discovered, whereas for this project additional research is unnecessary, as the technological advancements have already been established. The ISS has been occupied for over 16 years; taking into account an annual maintenance budget of approximately $5.2 billion gives the total maintenance cost of $83 billion, which justifies the BISS annual maintenance budget of $6.38 billion.

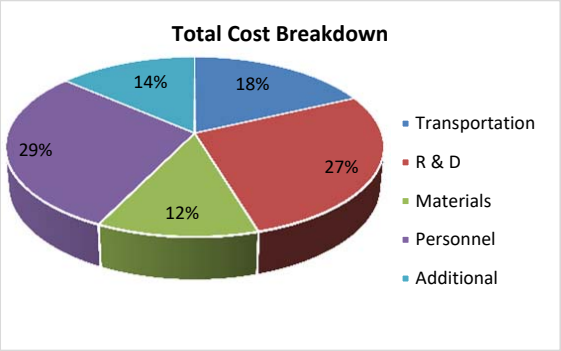

Fig. 15 BISS Total Cost Breakdown

VI. Conclusion

A review of multiple literature sources has enabled a detailed explanation of hazards associated with space exploration to be conducted. Techniques adopted from ISS and technological advancements in shielding from such hazards have been implemented into the spacecraft's design. A prototype design of the proposed space station was modelled using SolidWorks®, as displayed in Fig. 10; this incorporates shielding and protective technology. Constrained by economic limitations, comfort criteria have been applied to create artificial gravity of 3.711 m/s^2, which required the radius of the station to be 85 m. The size and rotational speed of BISS have been designed to remove the deleterious effect of microgravity and vertigo.

The SpaceX Falcon Heavy was selected as the suitable orbital launch system; this will be used to transport the approximate 675 ton space station into GEO, where it will be assembled. A structural analysis including simulations was carried out which located the main stress areas and ensured each component satisfied the factor of safety of 1.5. Compiling historical data allowed an approximate total cost of $47.039 billion for the entire BISS project to be calculated, this is significantly less than the current total cost of the ISS: $150 billion, this cost reduction is due to advances in orbital launch rocketry, manufacturing techniques and materials technology. Based on the data collected in this article it can be concluded that this project is feasible and affordable using currently available technology.

Appendix (I)

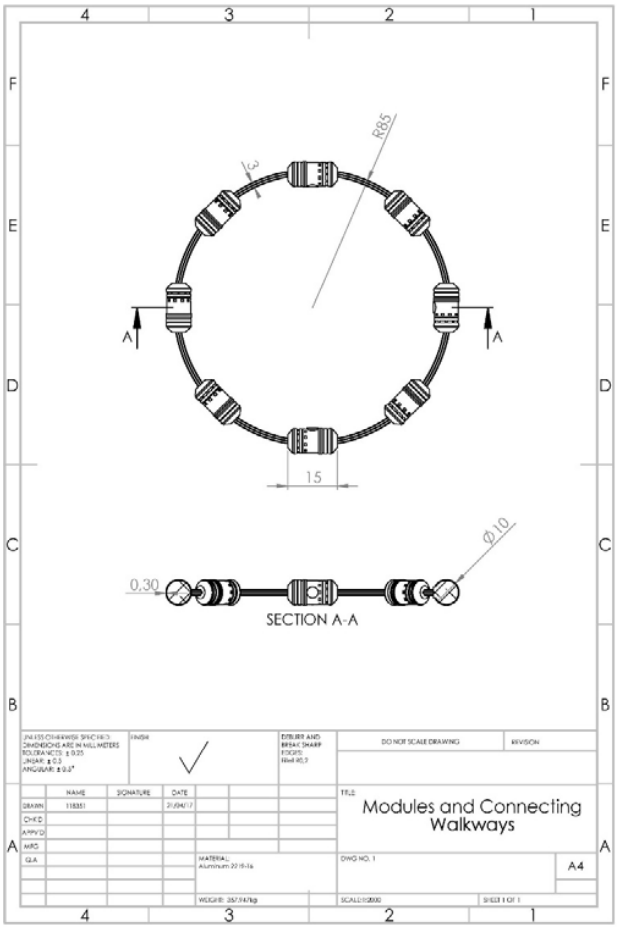

Fig. 16 Technical Drawing of Accommodation Modules and Connecting Walkways

Acknowledgment

This project was supported by the University of Sussex, United Kingdom.

References

[1] A. Siddiqi, Challenge to Appolo: The Soviet Union and the Space Race, Washington DC: NASA History division, 2000.
[2] D. J. Shayler, Walking in Space, New York: Springer: 2004 edition, 2004.
[3] L. J. DeLucas, "International Space Station," *Acta Astronautica* , vol. 38, no. 4- 8, pp. 61-619, 1996.
[4] R. Zimmerman, Leaving Earth: Space Stations, Rival Superpowers, and the Quest for Interplanetary Travel, Washington: Joseph Henry Press; 1st edition, 2003.
[5] S. B. Curtis, "Relating Space Radiation Environments to Risk Estimates," in *Biological Effects and Physics of Solar and Galactic Cosmic Radiation Part B*, New York, Plenum Press, 1993, pp. 817-830.
[6] R. Setlow, "The Hazards of Space Travel," *EMBO Reports,* vol. 4, no. 11, pp. 1-3, 2003.
[7] J. Curtis and S. B. Letaw, "Galactic cosmic rays and cell-hit frequencies outside the magnetosphere," *Adv. Space Red,* vol. 9, no. 1, pp. 293-298, 1989.
[8] P. Todd, M. Pecaut and M. Fleshner, "Combined effects of space flight factors and radiation on humans," *Mutat. Res,* vol. 3, no. 4, pp. 210-220, 1999.
[9] C. Poivey, "Radiation Hardness Assurance for Space Systems," *NASA*

GSFC, vol. 1, no. 1, pp 16-25, 2002.
[10] P. Fortescue, G. Swinerd and J. Stark, Spacecraft Systems Engineering, Oxford: Wiley; 4 edition, pp. 40-49, 2011.
[11] G. Clément, A. Bukley, W. Paloski, (2007) The Gravity Of The Situation. In: Clément G., Bukley A. (eds) Artificial Gravity. The Space Technology Library, vol 20, pp. 1-32. Springer, New York, NY
[12] J. V. Meck and et al, "Marked exacerbation of orthostatic intolerance after long - vs. short-duration spaceflight in veteran astronauts," *Psychosomatic Medicine,* vol. 63, pp. p 865-873, 2001.
[13] G. Glement, Fundamentals of Space Medicine 2nd ed, New Yord: Springer - Verlag New York, pp. 113 123 2011
[14] R. T. Jennings , "Treatment efficacy of intramuscular promethazine for space motion sicknes," *Aviat. Space Environ. Med ,* vol. 64, no. 3, pp. p 230 233, 1993.
[15] L. Young, Y. Kazuyoshi and W. Paloski, "Artificial Gravity Research To Enable Human Space Exploration," International Academy of Astronautics, Paris, 2009.
[16] T. W. Hall, "Artificial Gravity Visualization, Empathy, and Design," *2nd International Space Architecture Symposium,* vol. 19, no. 21, pp. 4-14, 2006.
[17] P. R. Hill and E. Schnitzer, "Rotating Manned Space Stations," *Astronautics,* vol. 7, no. 9, pp. 14-18, 1962.
[18] A. Graybiel, "Some Physiological Effects of Alternation Between Zero Gravity and One Gravity," in *Space Manufacturing Facilities (Space Colonies): Proceedings of the Princeton / AIAA NASA Conference May 7-9*, Reston, Virginia, American Institue of Aeronautics and Astronautics, pp. 137-149, 1977.
[19] J. R. Lackner and P. DiZIO, "Coordinated Turn-and-Reach Movements. I. Anticipatory Compensation for Self-Generated Coriolis and Interaction Torques," *Journal of Neurophysiology,* vol. 89, no. 2, pp. 276-289, 2003.
[20] Division on Engineering and Physical Sciences et al, Protecting the Space Station from Meteoroids and Orbital Debris, Washington, D.C.: National Academies Press, pp. 7-13, 1997
[21] D. J. Kessler et al, "Meteoroids and Orbital Debris," in *Space Station Program Natural Environment Definition for Design*, Houston, Texas, National Aeronautics and Space Administration pp. 155-168, 1994.
[22] E. L. Christiansen, "Design and performance equations for advanced meteoroid and debris shields," *International Journal of Impact Engineering,* vol. 14, no. 1-4, pp. 145-156, 1993.
[23] Inter-Agency Space Debris Coordination Committee, "IADC Space Debris Mitigation Guidlines," Steering Group and Working Group 4, 2007.
[24] L. J. Adams, "Principal Findings and Recommendations," in *Technology for Small Spacecraft*, Washington D.C., National Academy Press, pp. 17-20, 1994.
[25] J. N. Pelton, "The Space Debris Threat and the Kessler Syndrome," in *Space Debris and Other Threats from Outer Space*, New York, Springer, pp. 17-23, 2013.
[26] M. McKinnon, "A History of Garabage in Space," Gizmodo, 5th July 2014. (Online). Available: http://gizmodo.com/a-history-of-garbage-in-space-1572783046. (Accessed 15th April 2017).
[27] D. Mehrholz and L. Leushacke, "Detecting, Tracking and Imaging Space Debris," in *ESA Bulletin*, Paris, ESA, pp. 128-134, 2002.
[28] A. Rossi, E. M. Alessi and G. B. Valsecchi, "Disposal Strategies Analysis for MEO Orbits," University of Southampton, Southhampton, 2015.
[29] E. L. Christian, "Handbook for Designing MMOD Protection," NASA Johnson Space Center, Houston, pp. 44-44, 2009.
[30] M. Langford, "What is Space Radiation," *Space Radiation Analysis Group,* vol. 1, no. 1, pp. 1-1 2014.
[31] G. Walter and W. Barendsen, "Effects of Different Ionizing Radiations on Human Cells in Tissue Culture: IV. Modification of Radiation Damage," *Radiation Research,* vol. 21, no. 2, pp. 314-328, 1964.
[32] E. M. Soop, Handbook of Geostationary Orbits, New York: Springer; Softcover reprint of the original 1st ed, pp. 7-10 1994.
[33] S. K. Aghara, S. I. Sriprisan, R. C. Singleterry and T. Sato, "Shielding evaluation for solar particle events using MCNPX, PHITS and OLTARIS codes," *Life Sciences in Space Research,* vol. 4, no. 1, pp. 79-91, 2015.
[34] E. J. Hall, "Radiation Biolody for Pediatric Radiologists," *Alara Concept in Pediatric Imaging: Oncology,* vol. 1, no. 39, pp. 57-64, 2009.
[35] B. B. Ravinarayana et al, "Total Radiation Dose at Geostationary Orbit," *IEEE Transactions On Nuclear Science,* vol. 52, no. 2, pp. 530-534, 2005.
[36] P. L. Barry, "Plastic Spaceships," *NASA Science News*, 25 August 2005.
[37] A. T. Sheila et al, "Radiation Shielding Materials Containing Hydrogen,Boron, and Nitrogen: Systematic Computational and Experimental Study - Phase 1," Rochester Institute of Technology, New York, pp.17, 2012.
[38] D. Rapp, "Radiation Effects and Shielding Requirements in Human Missions to the Moon and Mars," *The International Journal of Mars Science and Exploration,* vol. 1, no. 2, pp. 46-71, 2006.
[39] M. M. Finchenor and D. Dooling, Multilayer Insulation Materials Guidelines, Alabama: NASA, pp. 1-4 1999.
[40] Space Studies Board et al, Space Radiation Hazards and the Vision for Space Exploration: Report of a Workshop, Washington, D.C.: National Academies Press, 2006.
[41] R. Nave, "Hyperphysics," 2017. (Online). Available: http://hyperphysics.phy-astr.gsu.edu/hbase/orbv.html. (Accessed 12th April 2017).
[42] Delft University of Technology, "ScienceDaily," ScienceDaily, 23rd May 2008. (Online). Available: www.sciencedaily.com/releases/2008/05/080521112119.htm. (Accessed 12th April 2017).
[43] E. J. O'Flaherty, "Modeling Normal Aging Bone Loss, with Consideration of Bone Loss in Osteoporosis," *Toxicotogical Sciences,* vol. 1, no. 55, pp. 171-188, 2000.
[44] A. W. Rupert, "Human Performance," in *The Cosmic Compendium: Space Medicine*, Raleigh, North Carolina, Lulu.com, 2015, pp. 1-7.
[45] S. M. Schneider et al, "Training with the International Space Station interim resistive exercise device," *Medical Science Sport Exercise,* vol. 11, no. 35, 2003.
[46] T. W. Hall, "Artificial Gravity and the Architecture of Orbital Habitats," *JBIS,* vol. 52, no. 7/8, pp. 290-300, 1999.
[47] M. V. Eerde, "Deriving the centripetal acceleration formula," Microsoft Developer, 24th January 2010. (Online). Available: https://blogs.msdn.microsoft.com/matthew_van_eerde/2010/01/24/deriving-the-centripetal-acceleration-formula/. (Accessed 13th April 2017).
[48] A. Dubrow, "Shields To Maximum," TACC, 25th June 2013. (Online). Available: https://www.tacc.utexas.edu/-/shields-to-maximum-mr-scott. (Accessed 20th April 2017).
[49] D. Kim, "Space Food," NASA, 25th November 2003. (Online). Available: https://spaceflight.nasa.gov/living/spacefood/. (Accessed 15th April 2017).
[50] T. A. G. Wood, "International Space Station's Solar Panels Have a No-Fail Mission," UrtheCast, 27th February 2012. (Online). Available: https://blog.urthecast.com/company/international-space-stations-solar-panels-have-a-no-fail-mission/. (Accessed 14th April 2017).
[51] R. R. King et al, "Advanced III-V Multijunction Cells For Space," Spectrolab, Hawaii, 2006.
[52] D. Estublier, S. Giorgio and A. Gonzalez, "Electric Propulsion," in *Electric Propulsion on SMART-1*, Noordwijk, esa bulletin, 2007, p. 45.
[53] D. M. Goebel and I. Katz, "Hall Thrusters," in *Fundamentals of Electric Propulsion: Ion and Hall Thrusters*, California, JPL Space Science and Technology Series, 2008, pp. 325-379.
[54] T. Trott, "Comparison of Orbital Launch Systems," Perfect Astronomy, 6th December 2013. (Online). Available: http://perfectastronomy.com/comparison-nasa-orbital-launch-systems/. (Accessed 20th April 2017).
[55] L. Allen, "U.S. Life-Cycle Funding Requirements," United States General Accounting Office, Washington D.C, 1998.
[56] S. L. Blum, Aerospace Cost savings - Implications for NASA and the Industry, National Academies, 1975.
[57] E. Gaddy, "Cost performance of multi-junction, gallium arsenide, and siliconsolar cells on spacecraft," in *IEEE Photovoltaic Specialists Conference*, Washington D. C., 1996.
[58] Indeed, "NASA Salaries in the United States," 12th April 2017. (Online). Available: April. (Accessed 18th April 2017).